Tumorigenesis and a DNA repair defect in mice with a truncating *Brca2* mutation

Frances Connor[1], David Bertwistle[1], P. Joseph Mee[2], Gillian M. Ross[3], Sally Swift[1], Elena Grigorieva[4], Victor L.J. Tybulewicz[2] & Alan Ashworth[1,5]

Germline mutation of the *BRCA2* gene carries a high risk of developing breast cancer. To study the function of this gene, we generated a mutation in *Brca2* in mice. Unlike other mutations in the *Brca2* gene, which are lethal early in embryogenesis when homozygous, some of our homozygous mutant mice survive to adulthood. These animals have a wide range of defects, including small size, improper differentiation of tissues, absence of germ cells and the development of lethal thymic lymphomas. Fibroblasts cultured from *Brca2*$^{-/-}$embryos have a defect in proliferation that may be mediated by over-expression of p53 and p21$^{Waf1/CIP1}$. We show that *Brca2* is required for efficient DNA repair, and our results suggest that loss of the p53 checkpoint may be essential for tumour progression triggered by mutations in *BRCA2*.

An estimated 5% of breast cancers are thought to result from a hereditary predisposition to the disease, primarily due to a small number of highly penetrant autosomally dominant genes[1,2]. Women who carry germline mutations in one of these susceptibility genes tend to develop cancer at an earlier age as well as being at an elevated risk of bilateral breast cancer and other cancers, such as ovarian cancer[3]. Two breast-cancer susceptibility genes, *BRCA1* and *BRCA2*, have been identified, and mutations in these genes are responsible for most cases in families with a large number of early-onset breast cancers[4–7]. Mutations in *BRCA1* are responsible for predisposition in the large majority of families with both breast and ovarian cancers, but account for only about half of the families with breast cancer only[3]. The *BRCA2* gene carries a risk of breast cancer similar to that of *BRCA1*, but is associated with a lower risk of ovarian cancer and a considerably higher risk of male breast cancer. However, despite the involvement of these genes in inherited cancer predisposition, no somatic, disease-causing mutations in either *BRCA1* or *BRCA2* have been reported in any breast cancer[8–11].

The *BRCA2* gene is widely transcribed, but at a relatively low level, and encodes a protein of 3,418 amino acids[7,12]. More than 70 independent mutations have been found in *BRCA2* in breast-cancer families; most of these are nonsense or frame-shift mutations, resulting in truncation of the protein[7,9–13]. The BRCA2 protein shows no strong homology to known proteins, but eight copies of a repeat have been identified in the region encoded by exon 11 (refs 14,15). Overall, the gene is poorly conserved in mammals, with only 59% amino-acid identity between mouse and human BRCA2 proteins[16,17].

BRCA1 and *BRCA2* have a number of similarities. The genes appear to be co-regulated both in the cell cycle and in different tissues of the adult mouse[16,18,19]. Furthermore, both proteins appear to interact with RAD51 (refs 20,21), the eukaryotic equivalent of the bacterial recombination protein recA, which has been implicated in repair of double-stranded DNA breaks[22,23]. Thus, it is feasible that BRCA1 and BRCA2 have a role in DNA repair. Both proteins also have domains that can function as transcription activation modules[24,25]; together with the demonstration that BRCA1 can associate with RNA polymerase-II holoenzyme[26], this suggests that the proteins might be involved in transcriptional regulation.

There have been several reports describing early embryonic lethality of homozygous mutations in *Brca2* in mice[21,27,28]. Here we describe a mutation in *Brca2* that probably leads to a partial loss of function of the gene. This provides a model of cancer caused by loss of the *Brca2* gene and has enabled the direct demonstration of a role for *Brca2* in DNA repair.

Targetted disruption of *Brca2*

We introduced a mutation into the mouse *Brca2* gene by homologous recombination in embryonic stem (ES) cells. The *Brca2* targetting vector was designed to insert a PGK-neo^r expression cassette, in the same orientation relative to *Brca2* transcription, into a *PstI* site in exon 11 at nucleotide position 6038 (ref. 16; Fig. 1). The targetting vector was electroporated into 129/Sv D3 ES cells, and 480 clones doubly resistant to G418 and ganciclovir selection were isolated and screened for disruption of the *Brca2* gene by Southern-blot analysis (Fig. 1). Three targetted clones with a euploid karyotype were subjected to extensive Southern-blot analysis to confirm correct disruption at one *Brca2* allele and that no additional random integrations had occurred (data not shown).

Blastocyst stage C57BL/6 embryos were injected with two of the targetted ES-cell clones. Five male chimaeric mice, three derived from one clone and two from a second clone, transmitted the mutated *Brca2* allele to their offspring. Chimaeras were mated with C57BL/10 (B10), F1 from a cross of C57BL/6 × DBA/2 (B6/DBA) or 129/Sv (129) females. To date, no phenotypic differences have been seen between mice generated from the two independently targetted ES-cell clones. A detailed analysis of one of these lines (B354) is presented here. Mice heterozygous for the *Brca2* mutation appear normal,

[1]*CRC Centre for Cell and Molecular Biology and* [5]*Section of Gene Function and Regulation, Chester Beatty Laboratories, The Institute of Cancer Research, Fulham Road, London SW3 6JB, UK.* [2]*Division of Cellular Immunology and* [4]*Division of Developmental Neurobiology, National Institute for Medical Research, The Ridgeway, Mill Hill, London NW7 1AA, UK.* [3]*Academic Radiotherapy and Oncology Unit, The Institute of Cancer Research, and Royal Marsden Hospital NHS Trust, Sutton, Surrey SM2 5NG, UK. Correspondence should be addressed to A.A. e-mail: alana@icr.ac.uk*

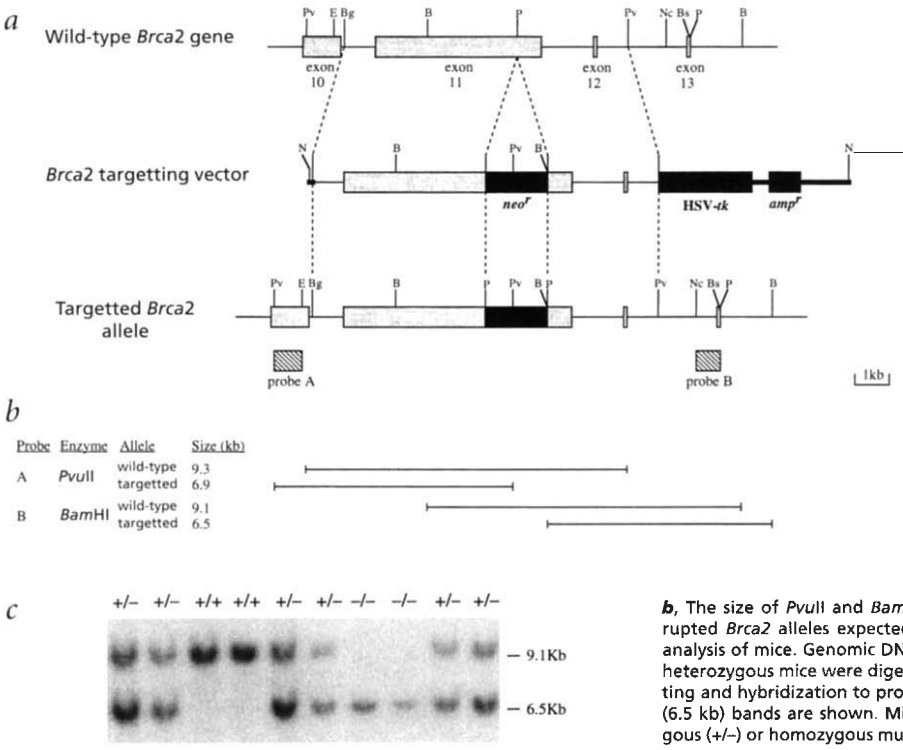

Fig. 1 Modification of *Brca2* in the mouse germ line. ***a***, Maps of the *Brca2* targetting vector linearized at a unique *Not*I site (middle) and the predicted structures of wild-type (top) and targetted (bottom) genes. *Brca2* genomic sequence is depicted as a thin line, with shaded boxes representing exons 10, 11, 12 and 13; the precise location of exon 12 is not known. Sequences from the pPNT plasmid and derived from pBluescript polylinker during construction are shown as thick lines, with filled boxes representing the neomycin resistance cassette (*neo*^{r}), the herpes-simplex-virus thymidine kinase cassette (HSV-*tk*) and the ampicillin resistance gene (*amp*^{r}). The *neo*^{r} and *Brca2* genes are transcribed in the same direction. *Brca2* genomic fragments, used as probes for Southern-blot analysis, are depicted as hatched boxes (probes A and B) positioned relative to the map of the targetted *Brca2* allele. Relevant restriction sites shown are *Bam*HI (B), *Bgl*II (Bg), *Bst*EII (Bs), *Eco*RV (E), *Pst*I (P), *Pvu*II (Pv), *Nco*I (Nc) and *Not*I (N). ***b***, The size of *Pvu*II and *Bam*HI genomic fragments from wild-type and disrupted *Brca2* alleles expected to hybridize to probes A and B. ***c***, Genotype analysis of mice. Genomic DNA from tails of 12-day-old progeny of a cross of heterozygous mice were digested with *Bam*HI and analysed by Southern blotting and hybridization to probe B. The sizes of wild-type (9.3 kb) and mutant (6.5 kb) bands are shown. Mice were identified as wild type (+/+), heterozygous (+/–) or homozygous mutant (–/–).

healthy and fertile for at least twelve months on the mixed 129/B10 or 129/B6/DBA genetic background or at least ten months on an inbred 129 background. In particular, no evidence of tumour formation in any of these mice has been observed.

Some *Brca2*$^{-/-}$ animals are viable

Mice heterozygous for the targetted *Brca2* disruption were intercrossed and offspring genotyped by Southern-blot analysis (Fig.1*b*,*c*). Live mice wild-type (*Brca2*$^{+/+}$), heterozygous (*Brca2*$^{+/-}$) and homozygous (*Brca2*$^{-/-}$) for the *Brca2* mutant allele were detected immediately after birth in the offspring on the 129 inbred and mixed genetic background. In the cross with 129/B6/DBA genetic background, some of the *Brca2*$^{-/-}$ mice survived weaning and reached adulthood. Cumulative genotyping of litters born with this genetic background revealed that the ratios of +/+:+/–:–/– were 1:1.93:0.23 (Table 1). These ratios are significantly different from the expected 1:2:1 mendelian ratio, with a large deficit of viable *Brca2*$^{-/-}$ mice.

To further characterize the time of lethality of most of the *Brca2*$^{-/-}$ mice, we analysed embryos from heterozygous intercrosses at day 17.5 of gestation. Expected numbers of live *Brca2* homozygous mutants were observed on the 129/B6/DBA genetic background (Table 1). Preliminary analysis of E18.5 embryos suggests that there is little prenatal lethality on this background (data not shown). Thus it appears that some lethality occurs just before or just after birth, and of those animals that are born alive, many do not survive to weaning.

The mutations that have been noted previously in the *Brca2* gene in mice result in early embryonic lethality when homozygous[21,27,28]. One possible explanation for the less severe phenotype we observed in our *Brca2*$^{-/-}$ mice is that we have generated a hypomorphic allele due to the site of the insertion into the *Brca2* gene; potentially, our mice could produce a 2,014-amino-acid truncated Brca2 protein, whereas the other mutations could produce only approximately 450, 626 or 978 N-terminal fragments of the full-length 3,329-amino-acid protein. Antibodies against the N-terminal region of Brca2 that could resolve this are not yet available, but we have used RT-PCR to study the expression of *Brca2* in mutant animals (Fig. 2*d*). This demonstrates that the 5′ part of the *Brca2* RNA is present and correctly spliced in the brain of a *Brca2*$^{-/-}$ mouse. Specifically, this shows that parts of the *Brca2* gene, the 3′ end of exon 10 and the 5′ portion of exon 11, deleted in the other, more severe *Brca2*$^{-/-}$ mutants, are transcribed and may result in the production of a truncated Brca2 protein. Another possibility is that insertion of the *neo* gene into exon 11 forced alternative splicing, resulting in production of an altered protein containing the C-terminus of Brca2. We have, however, been unable to find such alternative splicing by RT-PCR analysis. Moreover, an antibody that detects the C-terminus of Brca2, predicted to be absent in the *Brca2*$^{-/-}$ mutant, does not detect bands of altered mobility in protein extracts (data not shown), suggesting that this part of the protein is not expressed.

Table 1 • Genotypes of offspring from crosses of mice heterozygous for the *Brca2* mutation

Age	Genetic background	Number of litters	Number of pups	Genotype +/+	+/–	–/–	unknown
E17.5	129/B6/DBA	9	67	13	36	18	0
1–18 days	129/B6/DBA	45	320	98	189 (1)	23 (10)	10
1–18 days	129/B10	32	201	68 (3)	121 (2)	3 (3)	9

Progeny from crosses of mice heterozygous for the *Brca2* mutation were genotyped either at 17.5 days gestation (E17.5) or before weaning (1–18 days after birth). Unknown represents pups that disappeared (presumed eaten by the mother) or had died; genotyping was not possible. Numbers in brackets represent pups of known genotype that died before weaning age.

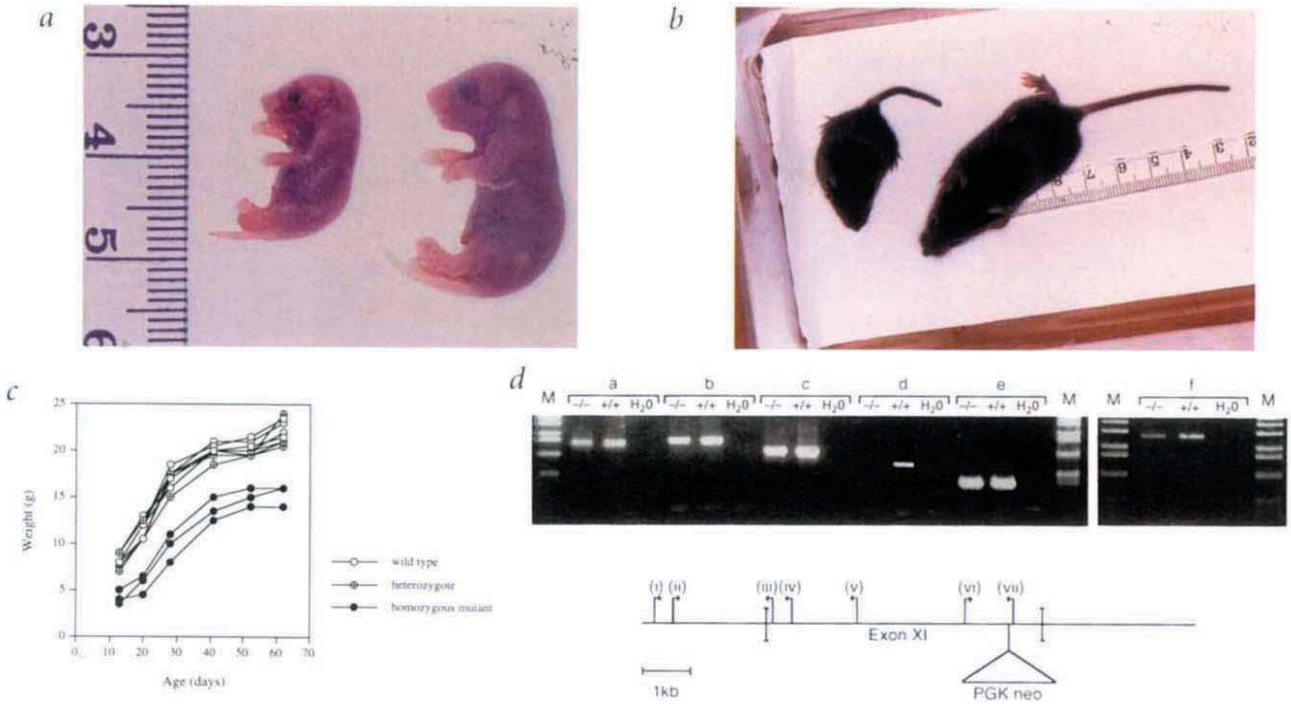

Fig. 2 Viability but growth impairment of some *Brca2*$^{-/-}$ mice. ***a***, E17.5 embryos from a cross of heterozygous mice. Left, *Brca2*$^{-/-}$ embryo; right, control littermate embryo. ***b***, Nineteen-day post-natum mice from a cross of heterozygous mice. Left, *Brca2*$^{-/-}$ mouse; right, control littermate. Note the kink in the tail of the *Brca2*$^{-/-}$ mouse. ***c***, The weight *versus* time of three surviving female *Brca2*$^{-/-}$ animals is shown compared to the growth curves of four heterozygous and three wild-type littermates. The growth curves of male *Brca2* mutant mice and their control littermates are similar to those shown. ***d***, The 5′ part of *Brca2* mRNA is expressed in *Brca2*$^{-/-}$ mice. mRNA was prepared from the brains of *Brca2*$^{+/+}$ and *Brca2*$^{-/-}$ mice. RT-PCR was used to amplify various portions of *Brca2* and *Hprt* cDNA. Primer combination vi and vii does not amplify a product in the *Brca2*$^{-/-}$ sample, as it is interrupted by the PGK-neo cassette. All other primer combinations, spanning multiple intron–exon boundaries, amplify *Brca2* cDNA from –/– samples and do not amplify a product from genomic DNA. Primer combinations and sizes are as follows: a) i and iii, 1,600 bp; b) ii and iv, 1,700 bp; c) ii and iii, 1,200 bp; d) vi and vii, 800 bp; e) Hprt f and Hprt r, 350 bp; f) ii and v, 3,100 bp. Positions of primers are indicated in the schematic and sequences given in Methods. The vertical bars indicate the boundaries of *Brca2* exon 11. Negative controls for the PCR amplification were performed by substituting H_2O for cDNA template. Amplified products were analysed on either a 1.5% (left panel) or a 1% (right panel) agarose gel. M indicates molecular weight markers (kilobase ladder, GIBCO).

Genetic background effect on *Brca2*$^{-/-}$ lethality

The *Brca2* mutation was introduced into the mouse genome by homologous recombination in the D3 ES-cell line originally derived from the 129/Sv strain[29]. Male chimaeras, in which the targetted ES-cell line had contributed to the germline, were initially crossed with either B10 females or F1 females from a cross of B6 and DBA. Progeny heterozygous for the *Brca2* mutation were then intercrossed to generate mice that could be *Brca2*$^{+/+}$, *Brca2*$^{+/-}$ or *Brca2*$^{-/-}$ and with genomes derived from varying proportions of 129 and B10 strains or of 129, B6 and DBA strains (Table 1). As stated above, live homozygous mutant animals are generated on the 129/B6/DBA background but at a reduced expected frequency; 7.4% were *Brca2*$^{-/-}$ instead of the expected mendelian 25%. Of these, only 4.3% survive to adulthood. The cross of heterozygotes with a 129/B10 background, however, generated only a few (1.6% instead of the 25% expected) *Brca2*$^{-/-}$ individuals, and they all

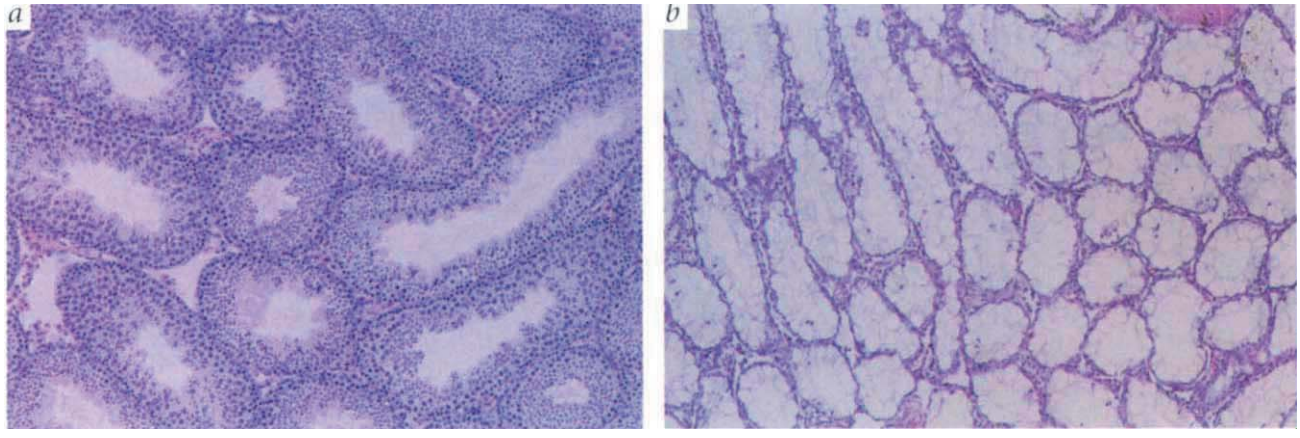

Fig. 3 Spermatogenic failure in *Brca2*$^{-/-}$ adult males. Sections of adult testis of male mice stained with haematoxylin and eosin showing seminiferous tubules (×400). ***a***, Heterozygote. ***b***, Homozygous mutant. Germ cells are absent from the seminiferous tubules of the homozygous mutant animal.

died within a few days of birth. Thus, we observed a genetic background effect on the lethality of the *Brca2* mutation.

Abnormal development of *Brca2*$^{-/-}$ embryos and adults

Male and female *Brca2*$^{-/-}$ mice are approximately half the weight of their littermates at embryonic stage E17.5, at birth, during nursing, at weaning age and as adults (Fig. 2). Another obvious abnormality is the presence of a distinct kink in the tail (Fig. 2*b*). This was seen in about 60% of individuals, but the extent varied considerably between individuals. This defect may be related to abnormal development of skeletal structures—including the ribs and sternum, which was observed at E14.5 (data not shown). Preliminary histopathological analysis has revealed that these animals also display numerous other defects. Examination of E17.5 mutant embryos showed that all organs are present; however, they appear to be significantly developmentally immature compared to those of age-matched controls. Also, some tissues show signs of improper differentiation. For example, the skin from an E17.5 mutant embryo shows a number of anomalies, including abnormal epidermal layering with a virtual non-appearance of the stratum corneum layer, poor stratification in the stratum spinosum and an ill-defined basal layer (data not shown).

Failure of spermatogenesis in *Brca2*$^{-/-}$ testes

Attempts to breed three adult male *Brca2* homozygous mutant mice were unsuccessful. The reproductive organs of these animals appeared to be grossly normal, except that the testes were much smaller than those of wild-type. Histological sections of adult control testes show seminiferous tubules containing Sertoli and spermatogonial stem cells at the periphery of the tubule and more differentiated cells towards the lumen, into which the mature spermatozoa are finally released. The seminiferous tubules of *Brca2*$^{-/-}$ testes contain Sertoli cells but, in contrast, appear completely devoid of germ cells and contain cellular debris (Fig. 3). The absence of spermatocytes indicates that the block in spermatogenic cell development is earlier than meiosis. The mutant germ cells may not colonize the gonads during embryogenesis or alternatively, after birth, spermatogonia may fail to proliferate. In either case, this would lead to an apparent absence of such cells in the adult. The ovaries of adult *Brca2*$^{-/-}$ females are also reduced in size, appear to be degenerating and have no obvious follicles (data not shown).

High frequency of malignant thymic lymphomas

To date, no *Brca2* homozygous mutant has survived beyond 5.5 months of age. Wild-type and heterozygote littermates of each mutant fail to develop any tumour or illness within the same period (Fig. 4*a*). The onset of disease symptoms—generally, weight loss, breathing difficulties and bulging sternum—occurred rapidly in six mutant animals (four males and two females) between the ages of 11 and 22 weeks (Fig. 4*a*). Examination revealed the presence of a grossly enlarged thymus, almost filling the chest cavity. These tumours completely lack the cortical-medullary organisation of the normal thymus and appear to be composed of uniform lymphoblastic-type cells (Fig. 4*b*). Flow-cytometric analysis suggests that the tumours originate from the immature CD4$^+$ CD8$^+$ double-positive thymocyte population and contain rapidly dividing cells with an activated phenotype (data not shown). Infiltration of the spleen with tumour cells emanating from the thymus was also observed.

Brca2$^{-/-}$ MEFs over-express p21 and p53

To determine whether the small size of *Brca2*$^{-/-}$ embryos and adults reflected a defect in cell proliferation, we compared the growth of wild-type, heterozygous and homozygous mutant mouse embryonic fibroblasts (MEFs) in culture. *Brca2*$^{+/-}$ and *Brca2*$^{+/+}$ MEFs proliferate well in culture whilst *Brca2*$^{-/-}$ MEFs proliferate poorly (Fig. 5*a*). Absence of *Brca1* and *Brca2* in mice has been suggested to lead to upregulation of the mRNA for the cyclin-dependent kinase inhibitor p21 (refs 28,30). We determined the level of p21 expression in MEFs wild-type, heterozygous and homozygous for our mutation (Fig. 5*b*). The p21

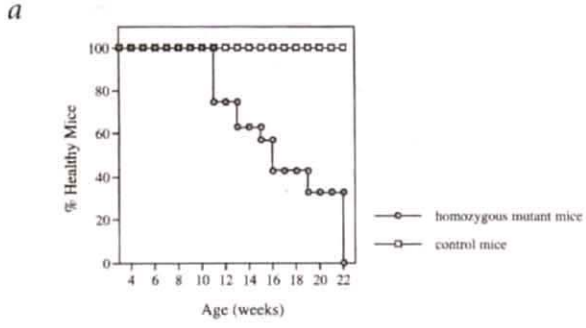

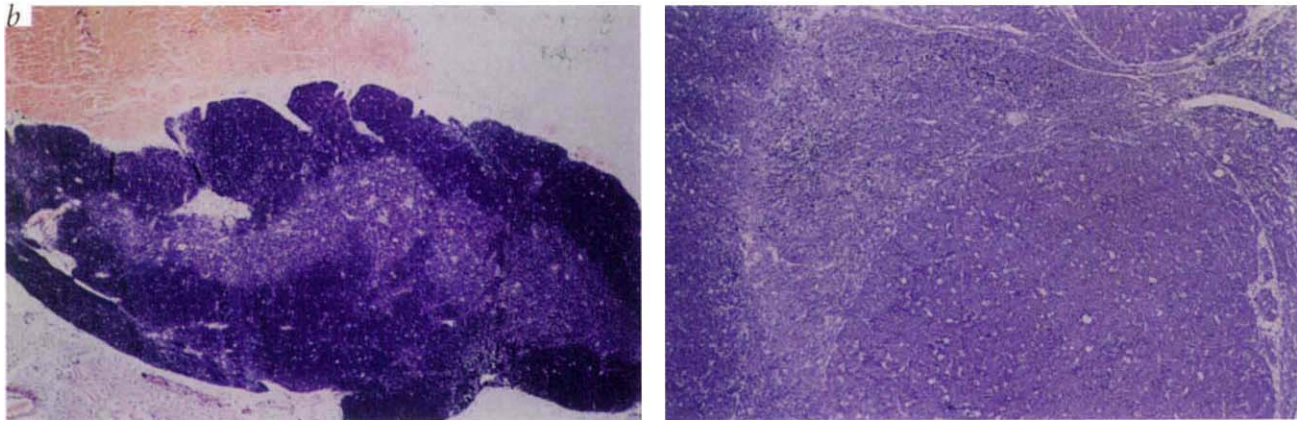

Fig. 4 High rate of mortality and thymic lymphoma in *Brca2*$^{-/-}$ mice. ***a***, Mortality of post-weaning *Brca2*$^{-/-}$ mice. The graph shows the percentage of healthy *Brca2* homozygous mutant mice and heterozygous and wild-type littermates plotted against age. Animals were killed as soon as they became obviously sick—with the exception of healthy wild-type and heterozygous littermates, culled as controls. Collection of data is ongoing; therefore, sample sizes (n) vary with age. For mutant animals, n is 11 (4–5 weeks), 8 (6–14 weeks), 7 (15–18 weeks) and 3 (19–22 weeks); for control animals, n is 42 (4–5 weeks), 29 (6–11 weeks), 27 (12–13 weeks), 26 (14 weeks), 23 (15–16 weeks), 22 (17–18 weeks) and 11 (19–22 weeks). ***b***, Photomicrographs of sections of normal thymus and thymic tumour from *Brca2*$^{-/-}$ mutants stained with haematoxylin and eosin (×40). Left, normal thymus showing differentiation into medulla and cortex; right, thymic tumour, greatly enlarged compared to normal thymus shown at same magnification and composed of uniform lymphoblastic-type cells.

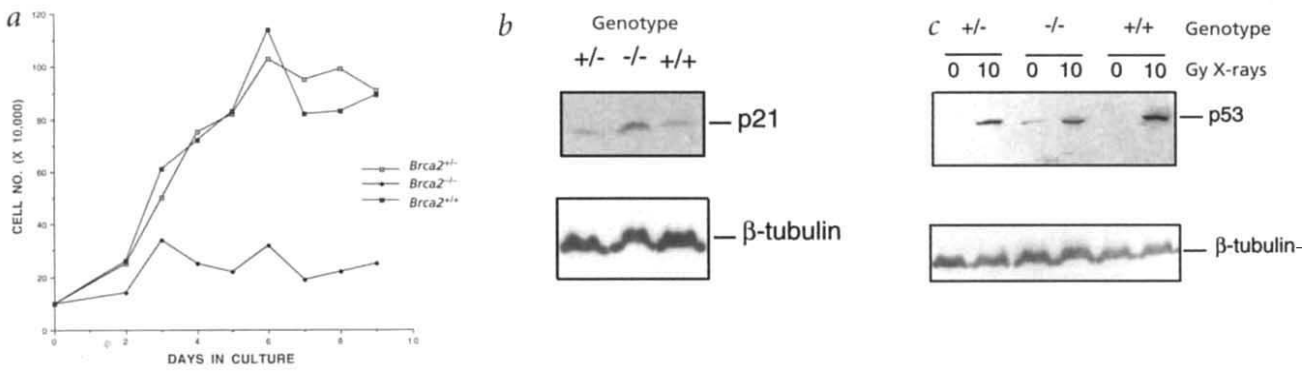

Fig. 5 Embryonic fibroblasts from *Brca2*$^{-/-}$ proliferate poorly in culture and overexpress p21 and p53. ***a***, *Brca2*$^{-/-}$ MEFs proliferate poorly. Proliferation curves of *Brca2*$^{-/-}$, *Brca2*$^{+/-}$ and *Brca2*$^{+/+}$ MEFs in culture. The cell number at each time point is the mean cell number of two duplicate plates. ***b***, *Brca2*$^{-/-}$ MEFs have elevated p21 protein levels. Western blot of lysates from *Brca2*$^{-/-}$, *Brca2*$^{+/-}$ and *Brca2*$^{+/+}$ MEFs were probed with the anti-p21 mouse monoclonal antibody, SX-118 and, as a loading control, an anti–β-tubulin antibody. ***c***, *Brca2*$^{-/-}$ MEFs have constitutively elevated p53 protein levels and can induce p53 in response to DNA damage. Western blot of lysates from *Brca2*$^{-/-}$, *Brca2*$^{+/-}$ and *Brca2*$^{+/+}$ MEFs, either untreated or irradiated with 10 Gy X-rays, were probed with the anti-p53 mouse monoclonal antibody, 421, and as a loading control, an anti–β-tubulin antibody.

protein is over-expressed in the *Brca2*$^{-/-}$MEFs. Given that p21 is an important target gene of the tumour suppressor p53, we measured p53 protein levels in the MEFs. Western-blot analysis demonstrated that p53 levels were consistently elevated in *Brca2*$^{-/-}$ MEFs relative to MEFs derived from littermate *Brca2*$^{+/-}$ or *Brca2*$^{+/+}$ embryos. Induction of p53 by X-irradiation appears not to be grossly impaired in *Brca2*$^{-/-}$ MEFs (Fig. 5*c*). This suggests that *Brca2* is not involved in sensing double-strand breaks, at least not upstream of p53.

DNA repair defect in *Brca2*$^{-/-}$ MEFs

To investigate whether *Brca2*$^{-/-}$ cells are competent for the repair of DNA damage, we subjected wild-type and *Brca2* mutant MEFs to 40 Gy of X-irradiation. A neutral, single-cell gel electrophoresis or, 'comet' assay,[32] was used to determine the relative amount of double-strand breaks in DNA present at various times after irradiation. *Brca2*$^{+/+}$ and *Brca2*$^{+/-}$ MEFs had repaired most double-strand breaks after 155 minutes, whereas *Brca2*$^{-/-}$ MEFs still showed considerable DNA damage, even after 275 minutes (Fig. 6). Thus, it would appear that *Brca2* is necessary for the efficient repair of double-strand breaks in DNA.

Discussion

Women carrying a mutation in either the *BRCA1* or *BRCA2* gene have a high risk of developing breast cancer[3]. Most of the mutations in *BRCA2* in humans that confer increased risk of cancer lead to truncation of the open reading frame (ORF) either by introduction of a nonsense codon or by a frameshift mutation[13]. We attempted to create a model of cancer induced by loss of *BRCA2* by introducing a mutation into the germ line of mice by homologous recombination. A *PGK-neo* cassette was introduced into exon 11 of the *Brca2* gene; this leads to the interruption of the ORF at amino acid 2,014 of the 3,329-amino-acid mouse Brca2 protein[16]. The mutant allele that we generated would be expected, if it occurred in humans, to confer an elevated risk of breast cancer; however, we have not so far observed tumours in mice het-

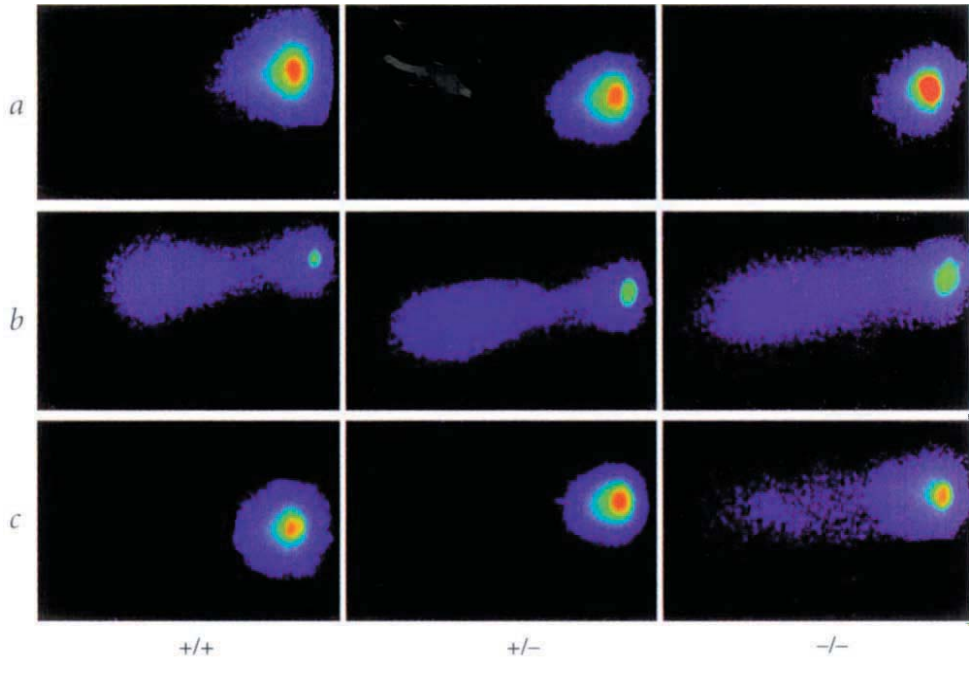

Fig. 6 Embryonic fibroblasts from *Brca2*$^{-/-}$ mice are defective in DNA repair. Neutral single-cell gel electrophoresis or 'comet assay' of *Brca2*$^{-/-}$, *Brca2*$^{+/-}$ and *Brca2*$^{+/+}$ MEFs either untreated (***a***) or irradiated with 40 Gy X-rays (***b***,***c***). Irradiated MEFs were harvested immediately (*b*) or after incubation at 37 °C for 275 minutes. Comet-tail length is proportional to the number of double-strand breaks present in the DNA of the cell. The cells shown have comet-tail lengths that are the median average for their data point.

erozygous for this mutation. Nor have tumours been observed in the *BRCA1* and *BRCA2* models of others[21,27,28,30,33,34]. This disparity may be due to a difference in the function of the genes between humans and mice. Alternatively, differences in breast development or physiology between the species might lead to the mutations being of very low penetrance.

Most mice homozygous for our *Brca2* muation die at or soon after birth, but just under one-third survive the perinatal period and reach adulthood (Table 1). Given that the other *Brca2* null animals previously described are severely affected and die between E6.5 and E8.5[21,27,28], the milder phenotype we observed suggests that we have generated a hypomorphic allele. This could be due to the position of insertion into the *Brca2* gene; the mice described here may produce a Brca2 protein that retains a large part of exon 11, which is predicted to be lacking in previously described Brca2 mutants. Of potential importance is our recent observation that the N-terminal part of exon 11 can bind to Rad51 (D.B. and A.A., manuscript in preparation) in addition to the previously reported C-terminal interaction domain present in Brca2 (ref. 21). Proof that we have generated a truncated version of the Brca2 protein awaits the generation of antibodies to the N-terminus of mouse Brca2, but RT-PCR analysis indicates that the mutant mRNA is stably expressed.

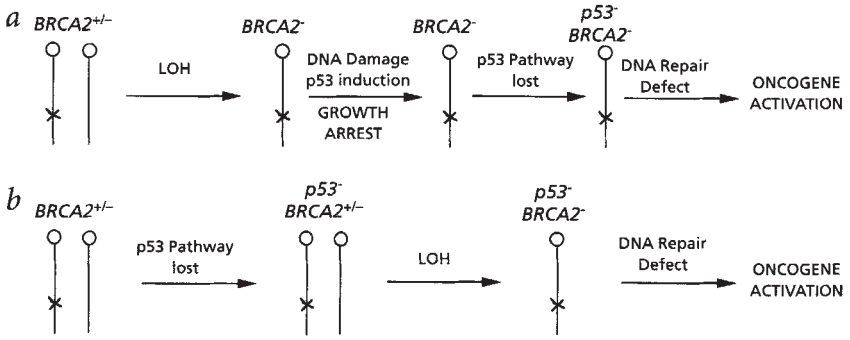

Fig. 7 Models for genetic changes in breast cancers in carriers of *BRCA2* mutations. ***a***, Loss of the wild-type *BRCA2* gene in a carrier of a *BRCA2* mutation leads to a defect in DNA repair. DNA damage results in induction of p53 and p21, which mediate growth arrest or apoptosis. Loss of the p53 pathway, by dominant-negative mutation of p53 or by other means, alleviates the growth arrest, allowing cell division. Failure of a DNA repair pathway leads to activation of oncogenes and neoplasia. ***b***, Cells carrying a heterozygous mutation in *BRCA2* lose the p53 pathway, by dominant-negative mutation of p53 or by other means. Loss of the wild-type *BRCA2* allele may be driven by a centrosome defect caused by loss of p53 function. Failure of a DNA repair pathway leads to activation of oncogenes and neoplasia.

It has been suggested that, in humans, modifying genes exist that affect the penetrance of mutations in *BRCA1* and *BRCA2* (ref. 3). For example, the same mutation in *BRCA2* in different Icelandic families is of variable penetrance, resulting in different distribution of cancers[35]. We show here that the mutation that we have introduced into the *Brca2* gene in mice has different effects, depending on the background strain. On a 129/B6/DBA background, we recovered some viable *Brca2*$^{-/-}$ mice, whereas all such mice on the 129/B10 genetic background die shortly after birth. This strain difference, if confirmed, should be useful in the identification of genes that modify the lethality of a *Brca2*$^{-/-}$ genotype. These genes may be of importance in modulating cellular responses to loss of the wild-type *BRCA2* allele in human carriers of *BRCA2* mutations and, hence, risk of developing cancer.

Fibroblasts derived from our *Brca2*$^{-/-}$ embryos have a defect in proliferation in culture, and this seems likely to be caused by over-expression of p53 and p21, which are known to mediate cell-cycle arrest. It has been noted that mice strongly expressing p53 die very early in embryogenesis[36,37]. In another study, ectopic expression of p53 in the kidney led to a failure in proper kidney differentiation[38]. Thus, the growth defects and the failure of several tissues to develop and differentiate properly that are observed in our *Brca2*$^{-/-}$ mice may be caused by inappropriate expression of p53. p53 is thought to be involved in maintaining the integrity of the genome and is activated in response to DNA damage, suggesting the presence of damaged DNA in the *Brca2*$^{-/-}$ fibroblasts. The previous observations that the Brca2 and Rad51 proteins interact and that *Brca2*$^{-/-}$ blastocysts are hypersensitive to gamma-irradiation implicate Brca2 in DNA repair[21]. Here we present further evidence that loss of Brca2 leads to a defect in DNA repair, leading to the accumulation of spontaneous DNA damage activating p53 and thereby p21.

A defect in DNA repair might also be the explanation for the development of thymic lymphomas in *Brca2*$^{-/-}$ mice. Lymphocytes mature through a process of DNA rearrangements of V(D)J gene segments involving double-stranded DNA breaks. The thymic lymphomas might be caused by a failure to repair these DNA breaks properly after V(D)J recombination. This could lead to an increased frequency of chromosomal translocations and inversions, which in turn could result in the activation of proto-oncogenes. We have not so far observed mammary tumours in *Brca2*$^{-/-}$ mice. This could be because the mice die of thymic lymphomas before the development of such tumours. Alternatively, and perhaps more likely, aberrant ovarian differentiation might lead to a hormonal deficit, resulting in reduced proliferation of mammary tissue.

In some respects, the phenotype of the mice that we have generated resembles that of mice null for the *Atm* gene[39–41]. *ATM* is the gene mutated in the inherited human disease ataxia-telangiectasia, whose phenotypes include growth retardation, elevated cancer risk and hypersensitivity to radiation[42]. Heterozygosity at *ATM* has been proposed to lead to a predisposition to breast cancer, although this is controversial[43–45]. Mice homozygous for a mutation in the *Atm* gene exhibit a reduction in size, germ-cell defects, failure of proliferation of embryonic fibroblasts and the presence of thymic lymphomas (in adult mice), phenotypes similar to those that we observed in the *Brca2*$^{-/-}$ mice. It is possible that the two genes act in the same biochemical pathway. Alternatively, it may be that most of the phenotypes in common are the result of defects in DNA repair either directly (germ cells, thymic lymphoma) or indirectly, due to low-level p53 expression (the growth defect, failure of proliferation of embryonic fibroblasts) as a result of DNA damage. In support of this conjecture, the failure of *Atm*$^{-/-}$ fibroblasts to proliferate in culture is rescued by a *p53*$^{-/-}$ background[46].

As discussed by others[47,48], the growth arrest in *Brca2* null cells is at odds with the suggested role of the gene as a tumour suppressor. Dominant-negative mutations in p53 or in another component of the p53 pathway would alleviate this arrest, allowing the cell to proliferate; this has been suggested to be the mechanism of escape from growth arrest[47–49] (Fig. 7*a*), and our data support this hypothesis. However, there is an alternative possible scheme (Fig. 7*b*). If a p53 mutation were to occur before loss of the wild-type allele, growth arrest would not occur, as the cell would still be *BRCA2*$^{+/-}$. This loss of p53 function could itself drive loss of the wild-type allele as p53$^{-/-}$ cells have been shown to undergo abnormal centrosome amplification, resulting in unequal segregation of chromosomes and aneuploidy[50]. This second potential order of events (Fig. 7*b*) might be a more plau-

sible mechanism for tumour development, as it does not envisage a growth-arrested stage. In either of these scenarios, other mutations, which perhaps activate dominant oncogenes, would then take place because of the mutagenic environment caused by the DNA damage driven by *BRCA2* loss. The mice described here should be useful in testing these various theories.

Methods

Construction of the *Brca2* targetting vector. Mouse *Brca2* sequences were isolated from a mouse 129/Sv genomic BAC library (Research Genetics) as described previously[16]. The *Brca2* gene targetting vector was made as follows. A 5-kb *Pst*I fragment containing the 3′ 0.65 kb of exons 11, 12 and 13 was subcloned into the *Pst*I site of pBluescriptKS. A 3.2-kb fragment (the 3′ 0.65kb of exon 11 and downstream sequence) was released by digesting at the polylinker *Bam*HI and genomic *Pvu*II sites and subcloned into the *Bam*HI and blunted *Eco*RI sites of the gene-targetting replacement vector pPNT[51] to yield the intermediate pPNT-3′ *Brca2* plasmid. A 5-kb *Bgl*II–*Pst*I *Brca2* genomic fragment (containing 4.2 kb of exon 11 and 0.8 kb of the preceding intron) was initially sub-cloned into the *Bam*HI and *Pst*I sites of pBluescriptKS. This fragment was released by digesting polylinker sequences with *Not*I and *Xho*I and then subcloned into *Not*I–*Xho*I–digested pPNT-3′ *Brca2* plasmid to give the *Brca2* targetting vector. The structure of the plasmid was confirmed by restriction mapping and by sequence analysis across the *Brca2*–PGKneo^r cassette junctions.

Gene targetting and generation of *Brca2* mutant mice. Gene targetting in ES cells was carried out essentially as described[52]. The *Brca2* targetting vector was linearized at a unique *Not*I site in the pPNT backbone and electroporated into D3 ES cells cultured on gelatin-coated dishes on a feeder layer of mitotically inactivated primary embryonic fibroblasts. After 9 days of selection with G418 (300 μg/ml) and ganciclovir (0.51 μg/ml), doubly resistant ES-cell colonies were isolated, expanded and frozen. The clones were screened for homologous recombination events by Southern-blot analysis of *Pvu*II-digested genomic DNA and hybridisation to probe A (Fig. 1*b*).

ES cells from *Brca2* targetted clones were karyotyped according to Robertson[53]. The correct structure of the targetted *Brca2* gene in cell lines with 40 chromosomes was confirmed by Southern-blot analysis of DNA digested with a range of restriction enzymes and hybridized with a neo^r probe and probes covering *Brca2* sequences present in and flanking the targetting vector (data not shown).

Chimaeric mice were produced by standard methods[54]. Euploid ES cells heterozygous for a correctly disrupted *Brca2* allele were injected into host C57BL/6 blastocysts, which were then transferred to the uteri of pseudopregnant (CBA×C57BL/10)F1 female foster mice. The resulting chimaeric mice, identified by agouti coat colour, were mated with C57BL/10 or (C57BL/6×DBA/2)F1 mice and, once germline chimaerism had been confirmed, 129/Sv mice. Heterozygotes were intercrossed to produce homozygous mutant mice. Mice were genotyped by Southern blotting of *Bam*HI-digested DNA, followed by hybridization with probe B (Fig. 1*b*) or by PCR. Genomic DNA was prepared from E14.5 and E17.5 embryo tissue or the tail tips of 1–3-week-old mice, essentially as described[52].

Phenotype analysis. Embryos were staged with the assumption that the day on which a vaginal plug was detected was E0.5. E17.5 embryos from heterozygous intercrosses were dissected free from the placenta and fetal membranes, blotted dry with a paper towel and weighed. Mice from heterozygous intercrosses were weighed during nursing (postnatal days 10–13), at weaning (days 20–23) and through to adulthood (days 40–47). After weaning, homozygous mutant mice were usually caged separately, while wild-type and heterozygous littermates of the same sex were housed together. In all cases, food and water were provided *ad libitum*. Embryos at E17.5 and adult mouse gonads were fixed in Bouin's fixative. Other adult tissues were fixed in 10% neutral buffered formalin. After fixation, samples were processed, embedded in paraffin, sectioned and stained with haematoxylin and eosin or Mallory's trichrome stain according to standard procedures.

RT-PCR. RNA was prepared and transcribed into cDNA, and *Brca2* fragments were amplified by standard techniques. The primers (Fig. 2*d*) were as follows. Forward primers: (i) exon 4, 5′–CAAAAAGAAGACCAAAGTGG–3′; (ii) exon 9, 5′–ATAGATCTGTTCCCTCAGTG; (vi) exon 11, 5′–CCGCCAGACATGAAGAATGC–3′. Reverse primers: (iii) exon 11, 5′–CCCAAAAGAGTTGGTCAAGG–3′; (iv) exon 11, 5′–TTTCACCAGGTGGCAGAAGC–3′; (v) exon 11, 5′–TTCTAACAGGTGAGGAAAGC–3′ (vi) exon 11, 5′–CACTTTCTGAAACTGTGACC. *Hprt* primers were (forward) 5′–GTCAAGGGCATATCCAACAACAAAC–3′ and (reverse) 5′–CCTGCTGGATTACATTAAAGCACTG–3′. PCR conditions were 30 s at 94 °C, 30 s at 52 °C and 2 min at 72 °C for 30 cycles, followed by 72 °C for 5 min. Reaction products were analysed on an agarose gel (1–1.5%) stained with ethidium bromide.

Culture of primary mouse embryonic fibroblasts. Primary mouse embryonic fibroblasts (MEFs) were derived from stage-E14.5 embryos from heterozygous intercrosses by standard procedures[53]. MEF cultures from each embryo were grown in DMEM supplemented with 10% fetal calf serum, 2 mM glutamine, 50 U/ml penicillin and 50 μg/ml streptomycin at 37 °C with 5% CO_2 until they reached confluence, when the cells were frozen (passage 1). Proliferation assays were performed as follows. Passage-2 MEFs were seeded into a series of 35-mm dishes at 1×10^5 MEFs per dish. Media were changed daily and cells counted from duplicate plates with a Coulter counter (Coulter Electronics). The assay was performed on two sets of MEFs, with similar results.

Analysis of p53 and p21 expression. MEFs isolated from *Brca2*$^{-/-}$, *Brca2*$^{-/-}$ and *Brca2*$^{+/+}$ embryos were seeded onto 10-cm dishes at 7×10^5 cells per dish. After one day in culture, dishes were irradiated with either 0 or 10 Gy X-rays (at a rate of 7.5 Gy/min). Media were changed immediately after irradiation. Total cell lysates were made by washing cells in PBS and addition, 2.5 h after irradiation, in RIPA buffer (50 mM Tris, pH 8.0, 130 mM NaCl, 0.1% SDS, 0.1% deoxycholate, 1% Triton X-100, 50 mM NaF, 1 mM sodium orthovanadate and ×1 complete protease inhibitors (Boehringer Mannheim). Protein content of lysates was determined with the BCA protein assay kit (Pierce). Each lysate (70 μg) was separated by 17.5% SDS-PAGE and blotted onto nitrocellulose. Blots were probed with the anti-p53 antibody, 421 or the anti-p21 antibody, SX-118 (gifts of X. Lu) and then incubated with an HRP-conjugated secondary antibody and developed with SuperSignal chemiluminescent substrate (Pierce). As a loading control, the blots were subsequently probed with an anti–β-tubulin antibody (N357, Amersham).

DNA damage and repair assay. Repair of DNA damage was analysed with a neutral single-cell gel electrophoresis (SCGE), or 'comet', assay. Neutral SCGE is specific for double-strand breaks in DNA. MEFs were seeded onto 55-mm dishes at 1×10^5 cells per dish and left overnight. The neutral comet assay was performed basically as described[32]. Monolayers of MEFs were harvested by trypsinization, and 5,000 cells were embedded in 1% low-gelling-temperature agarose (Sigma, type VII) at a final concentration of 0.7% agarose and pipetted onto fully frosted glass microscope slides (Dakin). After solidification of the agarose on ice, cell lysis was performed by incubation in 0.5% SDS, 30 mM EDTA and 0.25 mg/ml proteinase K (pH 8.0) (Boehringer Mannheim) at 4 °C for 1 h, followed by 37 °C overnight. Slides were rinsed in 0.5 × TBE before electrophoresis at 1 V/cm for 24 min at 10 °C in 0.5×TBE. Slides were stained with ethidium bromide (20 ng/ml) and visualized by epifluorescence with a Zeiss Axioskop microscope. Images were digitalized with the OPTIMAS image analysis software package. Fifty cells were analysed per data point, 25 from each of two duplicate slides. Tail length was calculated for each cell with the OPTIMAS software package. Median average tail length was calculated for each data point.

Acknowledgements

We thank the Cancer Research Campaign and the Institute of Cancer Research for financial support, X. Lu and R. Zamoyska for antibodies, M. Quinn and A. Walters for technical assistance and M. Turner, R. Zamoyska, P. Burgoyne and J. Martin for helpful discussions.

Received 24 October; accepted 5 November 1997.

1. Szabo, C.A. & King, M.-C. Inherited breast and ovarian cancer. *Hum. Mol. Genet.* **4**, 1811–1817 (1995).
2. Stratton, M.R. & Wooster, R. Hereditary predisposition to breast cancer. *Curr. Opin. Genet. Dev.* **6**, 93–97 (1996).
3. Easton, D. Breast cancer genes—what are the real risks? *Nature Genet.* **16**, 210–211 (1997).
4. Hall, J. M. *et al.* Linkage of early-onset familial breast cancer to chromosome 17q21. *Science* **250**, 1684–1689 (1990).
5. Miki, Y. *et al.* A strong candidate for the breast and ovarian cancer susceptibility gene BRCA1. *Science* **266**, 66–71 (1994).
6. Wooster, R. *et al.* Localization of a breast cancer susceptibility gene, *BRCA2*, to chromosome 13q12-13. *Science* **265**, 2088–2090 (1994).
7. Wooster, R. *et al.* Identification of the breast cancer susceptibility gene *BRCA2*. *Nature* **378**, 789–792 (1995).
8. Futreal, P.A. *et al.* BRCA1 mutations in primary breast and ovarian carcinomas. *Science* **266**, 120–122 (1994).
9. Lancaster, J.M. *et al. BRCA2* mutations in primary breast and ovarian cancers. *Nature Genet.* **13**, 238–240 (1996).
10. Miki, Y., Katagiri, T., Kasumi, F., Yoshimoto, T. & Nakamura, Y. Mutation analysis in the *BRCA2* gene in primary breast cancers. *Nature Genet.* **13**, 245–247 (1996).
11. Teng, D.H.-F. *et al.* Low incidence of *BRCA2* mutations in breast carcinoma and other cancers. *Nature Genet.* **13**, 241–244 (1996).
12. Tavtigian, S.V. *et al.* The complete *BRCA2* gene and mutations in chromosome 13q-linked kindreds. *Nature Genet.* **12**, 333–337 (1996).
13. Gayther, S.A. *et al.* Variation of risks of breast and ovarian cancer associated with different mutations of the *BRCA2* gene. *Nature Genet.* **15**, 103–105 (1997).
14. Bork, P., Blomberg, N. & Nilges, M. Internal repeats in the BRCA2 protein sequence. *Nature Genet.* **13**, 22–23 (1996).
15. Bignell, G., Micklem, G., Stratton, M.R., Ashworth, A. & Wooster, R. The BRC repeats are conserved in mammalian BRCA2 proteins. *Hum. Mol. Genet.* **6**, 53–58 (1997).
16. Connor, F. *et al.* Cloning, chromosomal mapping and expression pattern of the mouse *Brca2* gene. *Hum. Mol. Genet.* **6**, 291–300 (1997).
17. Sharan, S.K. & Bradley, A. Murine *Brca2*: sequence, map position, and expression pattern. *Genomics* **40**, 234–241 (1997).
18. Rajan, J.V., Wang, M., Marquis, S.T. & Chodosh, L.A. *Brca2* is coordinately regulated with *Brca1* during proliferation and differentiation in mammary epithelial cells. *Proc. Natl. Acad. Sci. USA* **93**, 13078–13083 (1996).
19. Vaughn, J.P. *et al.* Cell cycle control of BRCA2. *Cancer Res.* **56**, 4590–4594 (1996).
20. Scully, R. *et al.* Association of BRCA1 with Rad51 in mitotic and meiotic cells. *Cell* **88**, 265–275 (1997).
21. Sharan, S.K. *et al.* Embryonic lethality and radiation hypersensitivity mediated by Rad51 in mice lacking *Brca2*. *Nature* **386**, 804–810 (1997).
22. Game, J.C. DNA double-stranded breaks and the RAD50-RAD57 genes in Saccharomyces. *Semin. Cancer Biol.* **4**, 73–83 (1993).
23. Ivanov, E.L. & Haber, J.E. DNA repair: RAD alert. *Curr. Biol.* **7**, 492–4956 (1997).
24. Chapman, M.S. & Verma, I.M. Transcriptional activation by Brca1. *Nature* **382**, 678–679 (1996).
25. Milner, J., Ponder, B., Hughes-Davies, L., Seltmann, M. & Kouzarides, T. Transcriptional activation functions in BRCA2. *Nature* **386**, 772–773 (1997).
26. Scully, R. *et al.* BRCA1 is a component of the RNA polymerase II holoenzyme. *Proc. Natl. Acad. Sci. USA* **94**, 5605–5610 (1997).
27. Ludwig, T., Chapman, D.L., Papaioannou, V.E. & Efstratiadis, A. Targeted mutations of breast cancer susceptibility gene homologs in mice: lethal phenotypes of Brca1, Brca2, Brca1/Brca2, Brca1/p53, and Brca2/p53 nullizygous embryos. *Genes Dev.* **11**, 1226–1241 (1997).
28. Suzuki, A. *et al. Brca2* is required for embryonic cellular proliferation in the mouse. *Genes Dev.* **11**, 1242–1252 (1997).
29. Doetschman, T.C., Eistetter, H., Katz, M., Schmidt, W. & Kemler, R. The in vitro development of blastocyst-derived embryonic stem cell lines: formation of visceral yolk sac, blood islands and myocardium. *J. Embryol. Exp. Morphol.* **87**, 27–45 (1985).
30. Hakem, R. *et al.* The tumor suppressor gene *Brca1* is required for embryonic cellular proliferation in the mouse. *Cell* **85**, 1009–1023 (1996).
31. Lu, X. & Lane, D.P. Differential induction of transcriptionally active p53 following UV or ionizing radiation: defects in chromosome instability syndromes? *Cell* **75**, 765–778 (1993).
32. Ross, G.M. *et al.* DNA strand break rejoining defect in xrs-6 is complemented by transfection with the human Ku80 gene. *Cancer Res.* **55**, 1235–1238 (1995).
33. Gowen, L.C., Johnson, B.L., Latour, A.M., Sulik, K.K., Koller & B.H. Brca1 deficiency results in early embryonic lethality characterized by neuroepithelial abnormalities. *Nature Genet.* **12**, 191–194 (1996).
34. Liu, C.Y., Flesken-Nikitin, A., Li, S., Zeng, Y. & Lee, W.H. Inactivation of the mouse Brca1 gene leads to failure in the morphogenesis of the egg cylinder in early postimplantation development. *Genes Dev.* **10**, 1835–1843 (1996).
35. Thorlacius, S. *et al.* A single *BRCA2* mutation in male and female breast cancer families from Iceland with varied cancer phenotypes. *Nature Genet.* **13**, 117-119 (1996).
36. Montes de Oca Luna, R., Wagner, D.S. & Lozano, G. Rescue of early embryonic lethality in *mdm2*-deficient mice by deletion of p53. *Nature* **378**, 203–206 (1995).
37. Jones, S.N., Roe, A.E., Donehower, L.A. & Bradley, A. Rescue of embryonic lethality in Mdm2-deficient mice by absence of p53. *Nature* **378**, 206–208 (1995).
38. Godley, L.A. *et al.* Wid-type p53 transgenic mice exhibit altered differentiation of the uteric bud and possess small kidneys. *Genes Dev.* **10**, 836–850 (1996).
39. Xu, Y. *et al.* Targeted disruption of ATM leads to growth retardation, chromosomal fragmentation during meiosis, immune defects, and thymic lymphoma. *Genes Dev.* **10**, 2411–2422 (1996).
40. Barlow, C. *et al.* Atm-deficient mice: a paradigm of ataxia telangiectasia. *Cell* **86**, 159–171 (1996).
41. Elson, A. *et al.* Pleiotropic defects in ataxia-telangiectasia protein-deficient mice. *Proc. Natl. Acad. Sci.* **93**, 13084–13809 (1996).
42. Meyn, S. Ataxia-telangiectasia and cellular responses to DNA damage. *Cancer Res.* **55**, 5991–6001 (1995).
43. Swift, M., Reitnauer, P., Morrell, D. & Chase, C. Breast and other cancers in families with ataxia telangiectasia. *N. Engl. J. Med.* **316**, 1289–1294 (1987).
44. Fitzgerald, M.G. *et al.* Heterozygous ATM mutations do not contribute to early onset of breast cancer. *Nature Genet.* **15**, 307–310 (1997).
45. Bishop, D.T. & Hopper, J. AT-attributable risks? *Nature Genet.* **15**, 226 (1997).
46. Westphal, C.H. *et al.* Genetic interactions between atm and p53 influence cellular proiferation and irradiation-induced cell cycle checkpoints. *Cancer Res.* **57**, 1664–1667 (1997).
47. Kinzler, K.W. & Vogelstein, B. Gatekeepers and caretakers. *Nature* **386**, 761–763 (1997).
48. Brugarolas, J. & Jacks, T. Double Indemnity: p53, BRCA and cancer. *Nature Med.* **3**, 721–722 (1997).
49. Crook, T, Crossland, S., Crompton, M.R., Osin, P. & Gusterson, B.-A. p53 mutations in BRCA1-associated familial breast cancer. *Lancet* **350**, 638–639 (1997).
50. Fukasawa, K., Choi, T., Kuriyama, R., Rulong, S. & Vande Woude, G.F. Abnormal centrosome amplification in the absence of p53. *Science* **271**, 1744–1747 (1996).
51. Tybulewicz, V.L.J., Crawford, C.E., Jackson, P.K., Bronson, R.T. & Mulligan, R.C. Neonatal lethality and lymphopenia in mice with a homozygous disruption of the c-abl proto-oncogene. *Cell* **65**, 1153–1163 (1991).
52. Karaplis, A.C. *et al.* Lethal skeletal dysplasia from targeted disruption of the parathyroid hormone-related peptide gene. *Genes Dev.* **8**, 277–289 (1994).
53. Robertson, E.J. Embryo-derived stem cell lines. in *Teratocarcinomas and Embryonic Stem Cells: A Practical Approach* (ed. Robertson, E.J.) 71–112 (IRL, Oxford, 1987).
54. Bradley, A. Production and analysis of chimaeric mice. in *Teratocarcinomas and Embryonic Stem Cells: A Practical Approach* (ed. Robertson, E.J.) 113–151 (IRL, Oxford, 1987).